PRACE NAUKOWE Wyższej Szkoły Pedagogicznej w Częstochowie
Seria: FIZYKA z. V, 2002

I.V. KITYK[1], J. BERDOWSKI[1] J. EBOTHE[2]

[1]*Institute of Physics WSP, Al. Armii Krajowej 13/15, Częstochowa, Poland*

[2]*Universite de Reims, UFR Sciences, Unite de Thermique et d'Analyse Physique – LMET UPRES EA n°2061, 21 rue Clement Ader, 51865 Reims Cedex 02, France*

Anomalously Large Pockels Effect in ZnO-F Single Crystalline Films Deposited on Bare Glass

1. Introduction

Wurtzite-like ZnO single crystals have hexagonal symmetry (space group C_{6v}^4) and due to the lack of a centre of symmetry, they can have good properties described by the third order polar tensors. Particularly [1] have found a large electromechanical coupling caused by large piezoelectric effect, that is just used in industry. Interesting pressure-temperature anomalies of optical properties were found by [15]. On the basis of general phenomenological considerations, one can expect that these materials should also have good second-order non-linear optical properties. Of particular interest is the linear electro-optics effect (LEE), or Pockels effect described by the third-order polar tensor. LEE can be enhanced both through the use of film interfaces, as well as through appropriate doping. In order to find the appropriate doping, we applied a complex approach including theoretical band structure (BS) and molecular dynamics (MD) simulations.

To evaluate the non-linear optical susceptibilities, particularly the r_{ijk} tensor components of the electrooptics effect, as well as the influence on them of the interface and doping, carried out self-consistent band structure (BS) calculations of the perfect and doped ZnO crystalline films. A separate topics presents MD crystalline structure interface optimisation.

The techniques used in the specimen preparation and for the Pockels measurements are presented in Section 2. In Section 3, we present the results of the BS calculations together with the MD dynamics simulations of the interfaces. The results of the BS simulations, as well as the evaluated Pockels coefficients, are given in Section 4. We show that the Pockels effect is caused both by ZnO-glass interfaces, as well as by fluorine doping.

2. Experimental methods

2.1. Specimen preparation

The single ZnO crystalline films were deposited using a spray deposition technique from an aqueous solution made up of $ZnCl_2$ (Zn^{++} concentration = 0.05 M) for the pure ZnO sample. For the doped specimens, the appropriate solution was made up of $ZnCl_2$+NH_4F (same Zn^{++} conc.) for ZnO:F (6%).

The substrate temperature was about T = 450°C. The thin films investigated have a largely hexagonal-like structure and the preferred growth orientation was (002) axis normal to the bare glass substrate plane. The particular electron microscopy measurements have shown that doping does not change this orientation substantially.

Inhomogenuity was less than 7%. The crystallinity is very well defined due to the relatively high substrate temperature favouring the formation of pure material.

The reliability of the specimens was controlled on more than 200 specimens and the measurement statistic was reproduced within the 1.2%.

2.2. Measurements technique

The measurements of the LEE tensor coefficients were conducted using the traditional Senarmont method [3]. Light from a grating monochromator with wavelength range 380 – 900 nm and power of about 8 – 14 mW was used as the light source. The light intensity was stabilised within the 0.12%. The diameter of the laser beam was equal to about 1.5 mm. Λ/4 plate was used for detection of the crossed light. Precision of the birefringence evaluation was about 10^{-5}, making it possible to measure the LEE tensor component with accuracy of up to 0.005 pm/V. The grating monochromator's spectral resolution was approximately 0.4 nm/mm.

3. Molecular dynamics interface optimisation on the ZnO crystal – glass interfaces

Geometry optimisation of the film-glass interfaces plays a key role in understanding the origin of the effect described by third order polar tensors.

The structure and co-ordination bonding of the bare glass sheet touching the ZnO polycrystalline film were optimised using molecular dynamics (MD) structure optimisation. MD reconstruction of the glass Si-O sp^3 — bonds touching the ZnO wurtzite films was carried out.

The geometry optimisation of the reconstructed ZnO surfaces was started from the interface between the bare glass substrate and ZnO film sheet background. The optimisation was begun from the fourth neighbouring layers (two from the crystallite side and two in the direction of the bare glass substrate). About 50–60 atoms from both sides of the interface were taken into account. The MD procedure was carried out until the total energy minimum value for a given cluster was the same as for the whole cluster (re-normalised per one ion). At the second stage, the next crystalline layer of ZnO was considered, and the procedure was repeated for the new total energy per ion. The iteration process was repeated until the relative displacement of the ions for two successive layers was less than 0.2 Å. The latter one was limited by the framework of the adopted model. More details are presented in the [2].

The structure of the surrounding (near-the-interface ZnO) sheets was then additionally optimised using *ab initio* Car-Parrinello molecular dynamics (CPMD) [4] within a density functional theory (DFT) pseudopotential description. The functional used in the CPMD was of the Kleinman-Bylander type [5]. The atom core positions and the plane wave (PW) expansion coefficients were treated as simultaneous dynamic variables. Simulations in this approach were performed using super-cells containing 128 atoms with a PW cut-off of 37 Ry. Periodic boundary conditions and Γ point sampling of the Brillouin zone (BZ) were used. The calculated total energies using Γ (BZ) point were found to be accurate with precision better than 0.05 eV per atom. Martins-Trouiller pseudopotentials [6] in the Kleinmann-Bylander form were used to represent the Zn and O ion cores. This pseudopotential was verified for accuracy against silicon and germanium crystals.

At a PW cut-off of 40 Ry, the computed bond lengths agree with the experimental values. The so-called „liquid quench" method was applied to produce the final network at each bare glass configuration. The relative stability of the reconstructed interfaces was studied, in order to address the discrepancy between the experiment and existing DFT-LDA calculations. The performed by us evaluations have shown that the LDA approach underestimates the ZnO bulk lattice constant by 1.54%, and the pseudopotential approxima-

tion overestimates it by 0.18%. The best geometry corresponds to a lattice constant of about **a** = 3.259 A, **c** = 5.2081 A.

Our calculations have shown that the near-the-interface ZnO region may be considered like a reconstructed ZnO quantum confined surfaces deposited on the bare glass. The optimised structural ZnO data are presented in Table 1. Given that they are dependent on the distance from the ZnO layer-glass interface, the appropriate results are presented in relation to the distance d between the interface and actual ZnO layer.

TABLE 1. Changes in the effective structural parameters of the ZnO reconstructed surfaces during the shift from the interface (bare glass-ZnO crystallite) towards the deeper crystalline layers. The same parameters for the F-doped ZnO are given in brackets

Distance **d** from the glass – ZnO interface [nm]	**a**[nm], ZnO-6H (wurtzite structural component)	**c[nm]** (wurtzite structure)
0.2	2.889(4) (**2.872**)	5.515(2) (**5.523**)
0.4	2.916(3)(**2.912**)	5.486(1) (**5.493**)
0.6	2.937(1)(**2.935**)	5.450(6) (**5.458**)
0.8	2.956(5)(**2.955**)	5.412(4) (**5.416**)
1.0	2.974(4)(**2.973**)	5.378(2)(**5.381**)
1.2	3.002(2)(**3.002**)	5.267(3)(**5.268**)
1.4	3.112(4)(**3.112**)	5.134(9)(**5.134**)
1.6	3.251(1)(**3.251**)	5.209(3)(**5.209**)
1.8	3.258(6)(**3.257**)	5.2072(4)(**5.207**)
2.0	3.258(1)(**3.258**)	5.2071(0)(**5.207**)

One can see that the effective distance d for the Zn – O chemical bond shows considerable changes during the shift from the ZnO-glass interface towards the deeper ZnO layers. It is interesting that the ratio of the **c/a** increases with the shift towards the interface. An additional increase of this ratio is observed during the doping by fluorine.

For distances above 2 nm, the reconstruction of the ZnO wurtzite structure disappears and the bulk-like crystallite structure begins to dominate. In Figures 1–3 the differential local charge density distribution in relation to the distance **d** obtained by the method described above are presented. One can clearly see substantial charge density redistribution determining the electronic structure of the reconstructed ZnO surface. Because the thickness of the ZnO crystallites is relatively large (about 1000 nm), in our case one can propose a structural model similar to the ZnO wurtzite-like crystallites disturbed by bare glass.

In the Fig. 1–3 fragments of the local Zn –O charge density distribution for near-the-surface crystallites without doping (see Fig. 1 and Fig. 2), as well as after fluoridation, are presented (see Fig. 3). One can see that the interface causes substantial redistribution of the charge density electrostatic potential.

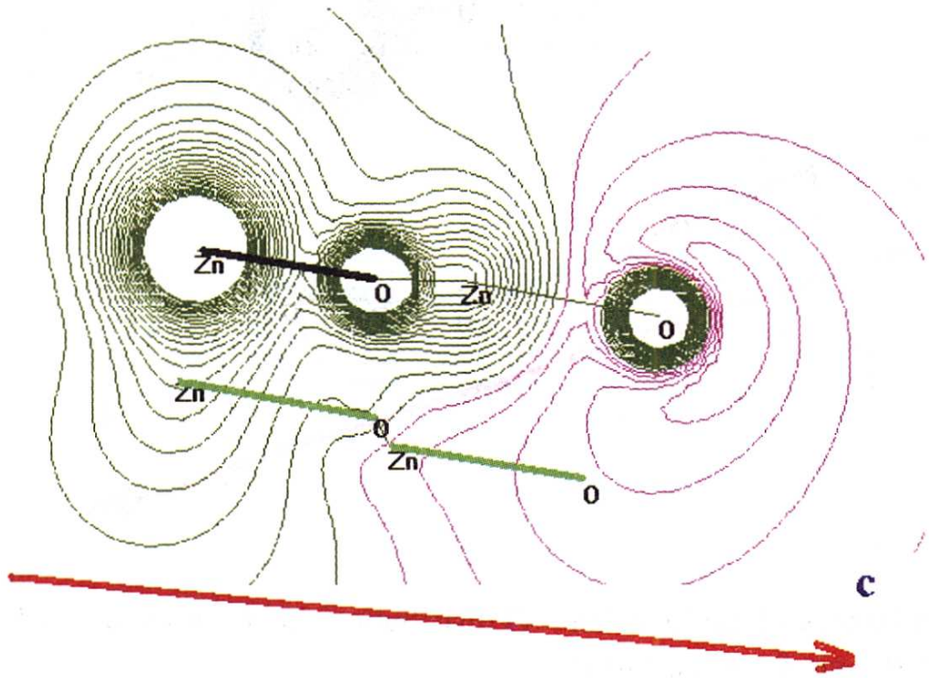

Fig. 1. Distribution of the electrostatic potential for the ZnO pure films 0.2 nm bear the bare glass interface before fluorine introduction

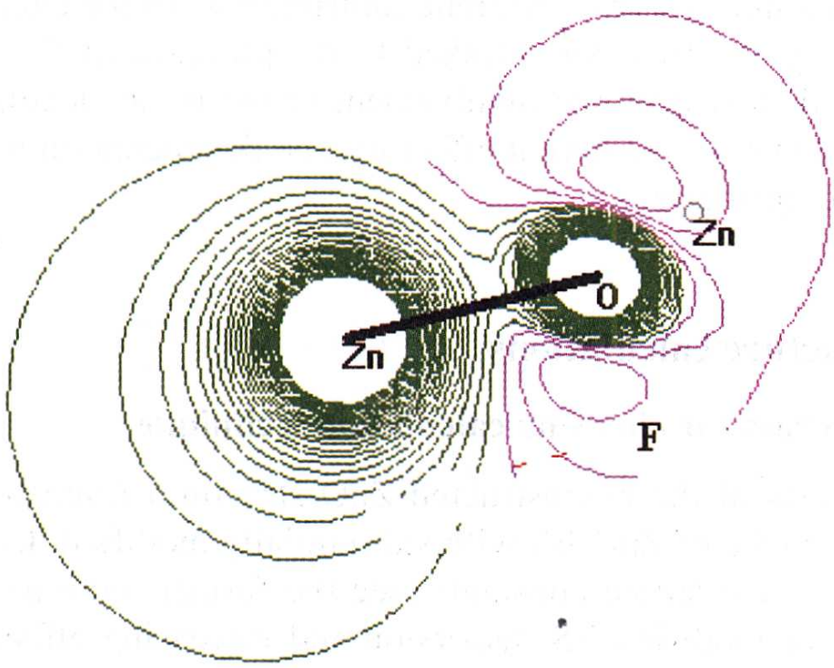

Fig. 2. Changes of local charge density distribution after introducing of the F for the deep ZnO crystallites (larger than 2 μm)

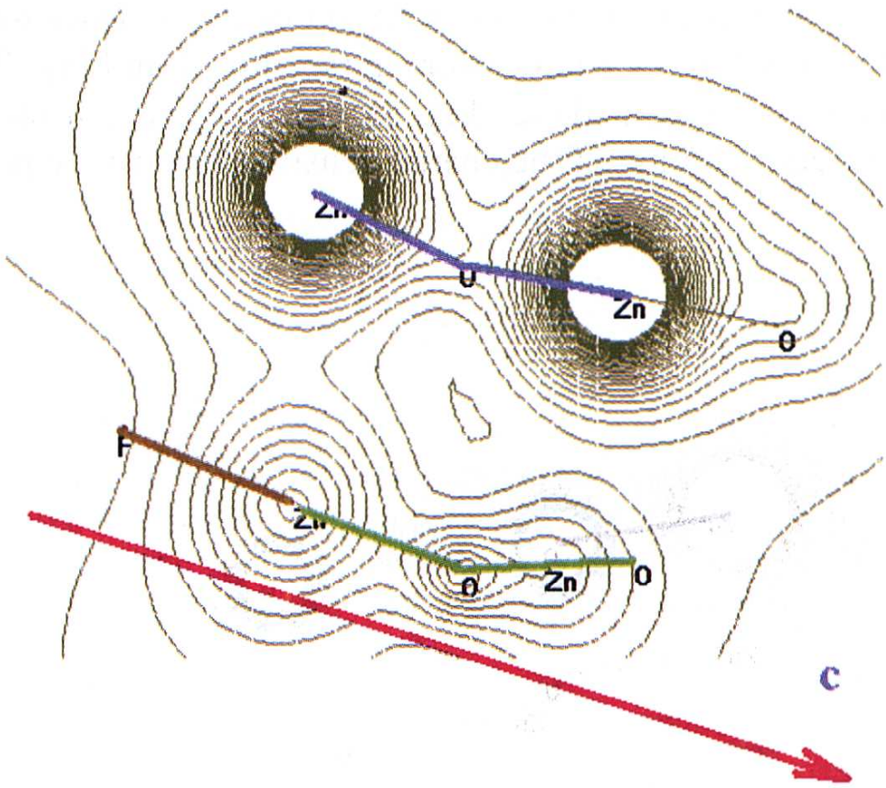

Fig. 3. Disturbances of the local Zn – O distribution due to influence of F at the distance about 0.2 nm from the surface

The distances Zn – O – Zn show additional non-centrosymmetry in the charge density distribution during the shift to the interface. Such disturbances in the structure indicate two different contributions to the charge density non-centrosymmetry, the first being linked to the presence of the ZnO^- interface, and the second caused by the involvement of the F ions leading to additional non-centrosymmetry. The output effect will be dependent on a sign and values of particular contributions.

4. Band structure calculations

4.1. Criterion for choosing calculation technique

On the basis of the reconstructed ZnO structural fragments, one can expect the appearance of ZnO BS with substantially modified **k**-dispersion. Due to varying effective lattice constants (see the former section) one can expect the existence of modified BS dispersion and increasing effective energy gap value.

There have been several works devoted to the BS calculations of perfect bulk ZnO crystals [7]. The choice of BS calculation technique depends on the kind of properties one wishes to simulate. As we were interested in simulations

of optical behaviour, our main criterion was to achieve maximum agreement between experimentally obtained optical parameters and those theoretically simulated. We therefore applied the following BS approaches: self-consistent full linear augmented plane wave approach within the local density approximation (FLAPW-LDA) [8,9], modified norm-conserving pseudopotential (NCPP) [3], semi-empirical pseudopotential methods (SEPM) [10]. These methods would seem to be the best of the BS calculation techniques available to date for interpreting optical data. Thus we will briefly perform comparison of the obtained data with experimental ones in order to choose the more effective to simulate the optical properties.

4.2. Norm-conserving pseudopotential method

The total energy of the crystalline system is expressed within a local density functional approximation (LDFA) with respect to the charge density ρ (**r**). Electrostatic and exchange-correlation effects were taken into account.

A nonlinear extrapolation procedure was carried out for evaluations of the weighting coefficients for the corresponding pseudo-wavefunctions, as well as the corresponding derivatives, in a form convenient for analytic evaluations of secular equation matrix elements, particularly:

$$\Psi(l,r,\beta)=\sum_n a_n^{\beta} r^n \exp\left[-\alpha_n^{(l,\beta)} r^n\right] \qquad (1)$$

where β denotes atom kind; l is the corresponding angular momentum; n determines the level of precision of the nonlinear fitting procedure and n can vary from 1 to 5. The coefficients a and α are fitting coefficients evaluated using non-linear fitting procedure with precision of the fit less than 0.03 eV.

The pseudopotential was chosen in the form:

$$V_{ps}^{(\beta,l)} = \sum_{i=1}^{3}\left[A_i^{\beta} + r^2 A_{i+3}^{\beta} \exp(-\alpha_l^{(l,\beta)} r^2)\right] \qquad (2)$$

This technique for calculation of matrix elements is described in detail elsewhere (see for example [2].

$$\left\|\left[\hat{\alpha}^2(\mathbf{k}+\mathbf{G}_n)^2/2m - E(\mathbf{k})\right]\delta_{n,n'} + \sum_{\beta} V_{\beta}(\mathbf{G}_n - \mathbf{G}_n) S_{\beta}(\mathbf{G}_n - \mathbf{G}_n)\right\| = 0 \qquad (3)$$

where E(**k**) is the eigenenergy for the **k**-point in the Brillouin zone (BZ), $\mathbf{G}_n$`,$\mathbf{G}_n$· are basis wavevectors of interacting basis plane waves. A structural

form-factors for the atoms of β kind were expressed as follows:

$$S_\beta(\mathbf{G}_n' - \mathbf{G}) = g^{(\beta)} / \Omega N_a \sum \exp\left(-\imath(\mathbf{G}_n' - \mathbf{G}_n)\tau_\beta\right) \tag{4}$$

where $g^{(\beta)}$ are weighting factor determining the partial contributions of the particular structural components (for every ZnO layers) to the total potential. A similar approach for different structural fragments has been successfully applied for binary solid alloys [11] glasses and organic materials [12,13]. One can expect that this approach may be appropriate also for different disordered and partially ordered solids including the ZnO and ZnO-F film interfaces investigated. As a consequence the reconstructed interface contribution is directly taken into account within the mentioned approach.

The special Chadhi-Cohen point method [8] was applied for calculations of spatial electron charge density distribution. Secular equation's diagonalization procedure was carried out at special weighting points of the BZ for each structural type.

Acceleration of the iteration convergence was achieved by transferring 84% of the (m–1)-th iteration result to the m-th iteration. The following condition was taken as a criterion for self-consistency:

$$\left|(\rho_m - \rho_{m-1})/\rho_m\right| < \varepsilon \tag{5}$$

During the self-consistent calculations, the level of calculation error (ε was no higher than 0.12%). To see whether the results of BS calculations depend on the choice of local structure optimisation, verifying calculations for the pure ZnO and doped ZnO-F crystalline wurtzite-like film layers were carried out. However, the main drawback of all one-electron local density functional-local density spin approach (LDF-LDSA) calculations consists in an underestimation of the band energy gap values. For this reason self-energy correction renormalisation was performed [15,16].

As a ZnO base BZ, a wurtzite-like hexagonal structure was chosen because this corresponds to the major structural component of the investigated films. Varying structural factors for the different layers and coming out from the structural data obtained using the MD geometry optimisation (see Table 1) the appropriate atomic positions were introduced in the structural factors (see Eq. 4).

To make the core-like state contributions more realistic, the norm-conserving PP wavefunctions were modified additionally through their orthogonalisation to the LCAO wavefunctions as described by [13]. As a result, the

total energy deviation during the self-consistent procedure in relation to the energy cut-off and the Perdew-Alder screening parameter was stabilised to 0.22 eV.

4.3. Local-density-derived semi-empirical pseudopotential (SEPM)

As a second method for calculations of the structures, we applied the modified semi-empirical pseudopotential (SEPM) approach introduced by [17,18]. This approach was proposed explicitly for quantum dots, wires, wells, and films–with typical linear dimensions of 2–10 nm. In our case, the thickness of the reconstructed ZnO layers was of the same order.

The SEPM approach is much faster than the self-consistent first-principle methods used for bulk solids. Indeed, the Schroedinger equation is solved and an efficient diagonalization method providing energy levels in a fixed „energy window" is available and appropriate. Unlike effective-mass-based approaches [16], this method uses *explicit* and variation flexible basis functions, permitting a direct comparison of wave functions with the LDF studies when available. However, unlike the LDF approach, the SEPM method provides only BS information, transition probabilities, wave functions but not the ground-state properties such as equilibrium structural geometry, which have to be assumed at the outset.

The general secular equation approach is similar to that described in chapter 4.2.1. In the scalar local-density approximation (SLDA) the scalar-relativistic atomic pseudopotential is obtained using the Troullier – Martins procedure [6] to perform the core-like correction. A PW basis with a kinetic energy cutoff of 32.5 Ry was applied. The non-local part of the ionic pseudopotential V was obtained numerically. It was kept unchanged during moving from the LDA to the SLDA. The "small box" implementation was applied to handle the nonlocal part of the pseudopotential. This approach takes an advantage of the short-range nature of nonlocal part, and uses the PW basis set with large momentum to expand it in Fourier space.

It is well known that the LDF band gaps are usually underestimated. These were therefore adjusted to reproduce the experimentally observed BS using self-energy corrections. The changes in the SLDA potentials are small compared with the LDA results. Our calculations showed that sufficient sizes of the secular matrix were achieved for the matrix sizes varying within the 120 – 260.

Since the final pseudopotential was rather smooth, a rapidly converged PW expansion was possible. In fact using the efficient diagonalization method and the full semi-empirical pseudopotential, the electronic structure of up to a 90-atom ZnO supercluster could be calculated.

4.4. FLAPW-LDA approach

Among the different BS calculation methods, the augmented plane wave (APW) methods are very popular. One of the well known is a version WIEN97 [19]. In the fully linear augmented plane wave local density approximation (FLAPW-LDA) and in accordance with the exchange-correlation Hedin-Lundquist parameterisation was carried out. The ZnO PW basis set was taken for the energy cut-offs of about 18 eV and potential representation about 61 eV. The expansion by angular-dependent spherical harmonics was done up to the $l<12$. About 24 states were taken into account including 6 empty states, with the criterion for the self-consistent eigenenergy value stabilisation about 0.012 eV. Summation within the BZ was performed at 12 special points of the BZ [14]. All the core states (*1sO, 1sZn, 2sZn,2pZn,3sZn, 3pZn,3dZn, 2sO,2pO*) were recalculated during each iteration step. The Thomas-Fermi screening potential was applied at the beginning, but was later successfully replaced by the Engel screened functions. Additional corrections using the generalised gradient approximation (GGA) [20] to prevent energy gap underestimation were undertaken.

The PW basis set was limited by wave vectors less than $9/R_m$ (R_m-muffin-tin sphere radius). The pure ZnO crystallites required 1110 plane waves and ZnO-F structural type needed 560. The radius of the Zn sphere was varied within the range $R_{Zn} = 1.06 - 1.21\ R_O$. The interacting spheres were chosen to be non-overlapping (only touching). As core states, *1s O* wavefunctions and *1,2 s,2p Zn* were taken. All the remaining orbital were considered as valence states orbital.

For numerical calculations of the total and partial density of states (DOS) numerical simulations by tetrahedron method using 128 **k** points with the energy resolution of 0.16 eV were carried out. The Zn, O and F atoms are relatively light and the spin-orbit interaction was not taken into consideration. For the classification of the BZ, the notation presented in Ref. 9 are given.

4.5. Results of the BS calculations

As an important criterion of an applicability of the concrete method, the structural (see Table 2) parameters calculated by the different methods are presented. One can see that maximum agreement between experimental and theoretically calculated data is given by a modified NCPP approach. The SEPM and FLAPW methods give results which substantially deviate from experimental findings.

Typical fragments of the BS dispersions calculated for ZnO wurtzite structure with and without fluorine modified by the near-the-interface structure are shown in Figures 4–5. One can see that for both methods, taking into account the reconstruction surfaces leads to substantial deviations in the band energy dispersions. Moreover in the case of the NCPP method (Fig. 5), we have a substantial shift in the effective top of the valence band and conduction bands.

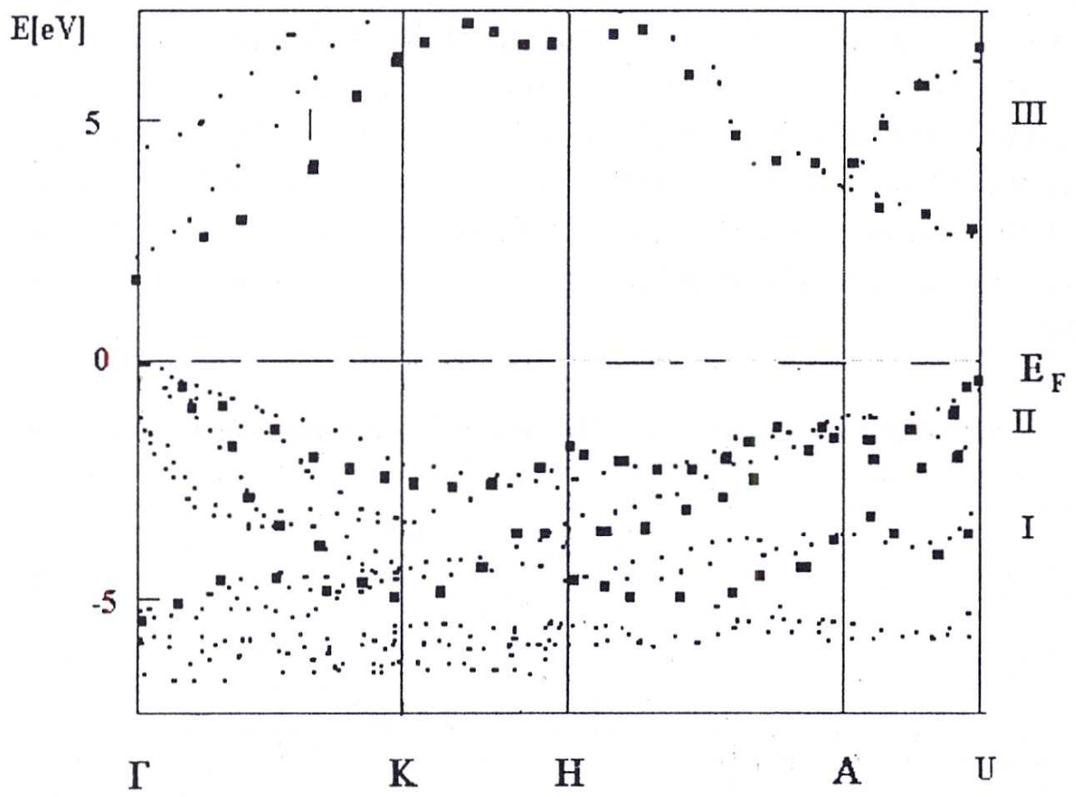

Fig. 4. Band structure of the ZnO policrystalline films with disturbance by an interface and fluorine (squares) calculated within the FLAPW method

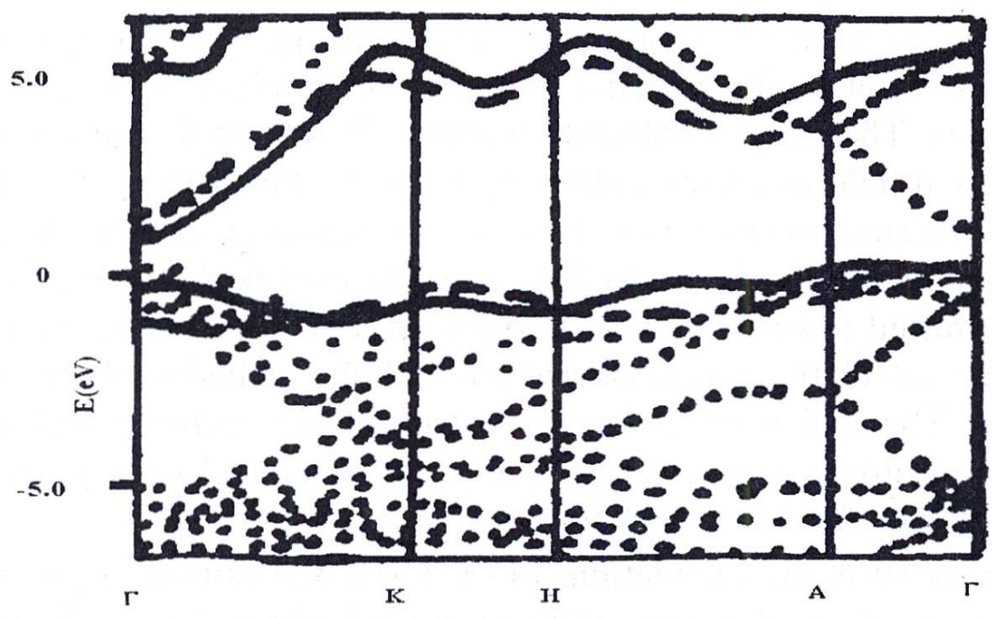

Fig. 5. Band energy structure of the ZnO crystalline films doped by F on the glass substrate calculated by NCPP method. By the solid line are indicated the deviations connected with the influence of substrate

The presentation is limited only by the NCPP as well FLAPW approaches because the SEPM data give results substantially different comparing with the experimental. One can see (cf. Fig. 4 and Fig. 5) substantial deviations of the BS dispersion from the BS for the pure ZnO wurtzite-like crystals. For convenience, we show only deviations for the top of the valence band and the bottom of the conduction band. The flatter bands suggest the particular role of the reconstructed near-the-interface structure in the observed band structure dispersion.

TABLE 2. Lattice constants for the 4H- and 3C-polytypes calculated by the different methods

	ZnO [A]	ZnO-F [A]
NCPP modified as in the present work	3.258	3.265
FLAPW-LDA	3.241	3.252
SEPM	3.223	3.242
Experimental [obtained from experimental diffraction	a=3.259; c=5.2081	a=3.263 A; c=5.2162 A

The modified NCPP method gave better agreement with experimental structural data. Thus it was chosen as base for the simulation of optical properties.

5. Dispersion of refractive indices and electrooptics coefficients

At the beginning, calculations of the imaginary part of dielectric susceptibility optical tensors were carried out in order to simulate linear and electrooptic properties. The general calculation approach was applied using the calculated matrix dipole moments obtained by the NCPP method. Additionally performed numerical verification showed that nonlocal effects change the average oscillator strength by up to 16%. The plasmon peak in the energy loss spectra was shifted towards higher energies up to 1.8 – 2.6 eV. As a consequence, all the calculations were carried out with the inclusion of the nonlocal contributions. The real parts of the dielectric tensors were evaluated using Kramers-Kronig dispersion relations. The reflectivity and energy loss functions were obtained from Fresnel's formula.

A crucial point in the calculations of the $\varepsilon_2(E)$ was caused by precision of the **k**-space integration. A linear tetrahedron method for the 312 **k** points in the 1/48 irreducible part of the BZ was applied. In the present paper, during the BS summation, 36 conduction bands were included in order to achieve converged results. This convergence is a crucial point for the calculation of the loss-electron spectra.

The calculated data make it possible to estimate changes in the refractive indices which correspond to the real part of $\varepsilon_2(E)$. On the basis of the general phenomenology, one can also expect substantial enhancement of the appropriate Pockels tensor components. The data calculated using this method is shown in Table 3.

TABLE 3. Evaluated values of the Pockels tensor components for different wavelengths

λ[nm]	r_{222}[pm/V]	r_{212}[pm/V]
750	4.81	2.18
700	4.89	2.31
650	5.01	2.52
550	6.01	2.84
500	7.56	3.01
450	10.6	3.86
400	15.2	4.01

On Table 3, one can see substantial anisotropy in the tensor component distribution. This reflects the specific contribution of interface and fluorine polarisation.

From Fig. 6 one can see that doping by fluorine favours an increase in refractive indices connected with the additional anisotropy in the charge density distribution. This fact reflects the particular role played by fluorine atoms in the variation of the refractive index perpendicular to the optical axes.

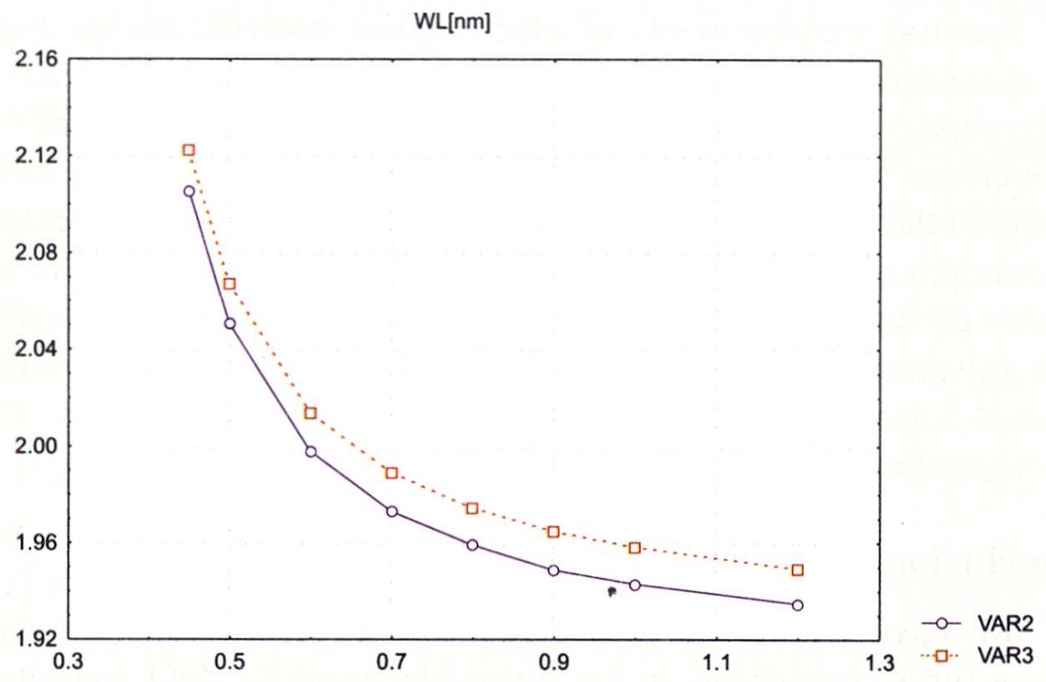

Fig. 6. Dispersion of ordinary refractive indeces for pure (o) and doped (□) crystallites

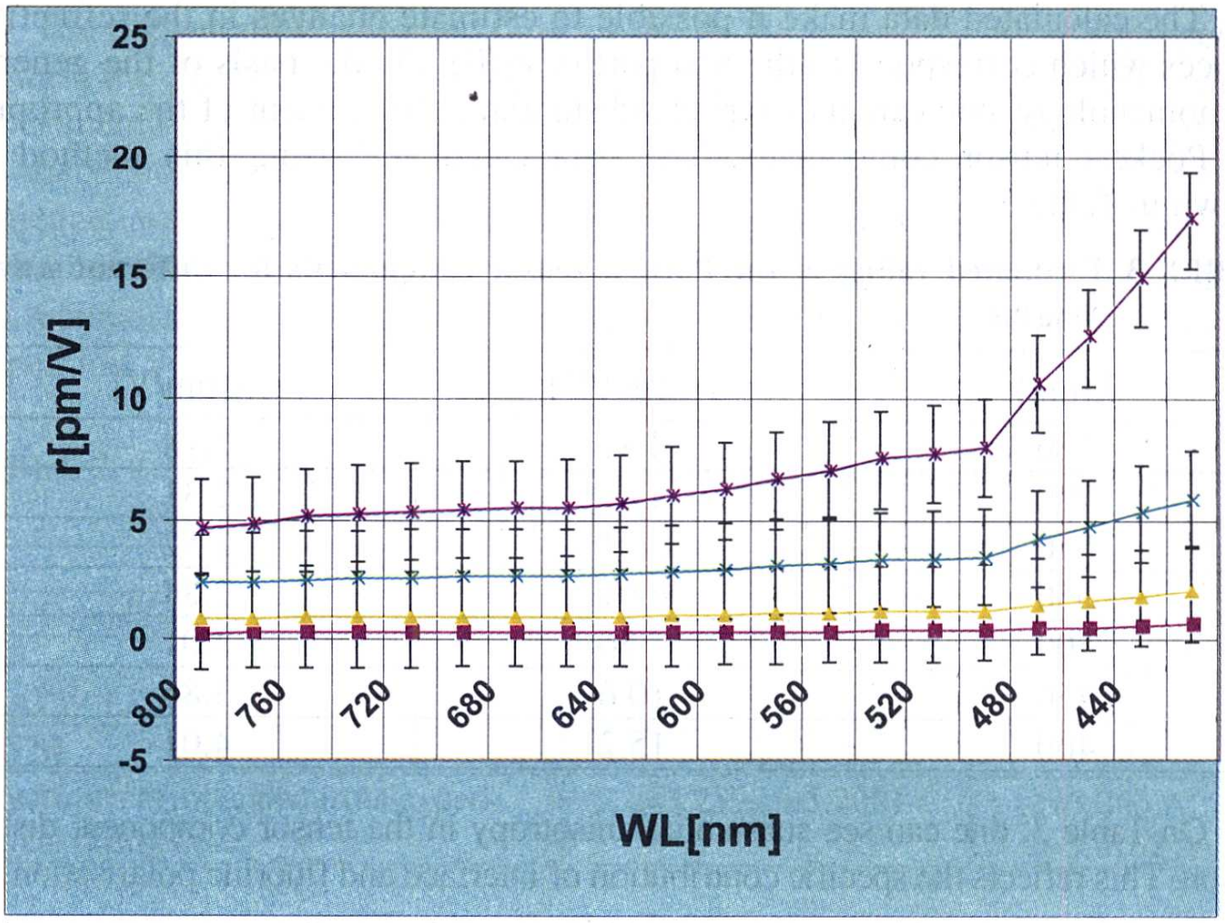

Fig. 7. Spectral dependences of the r_{222} for: ■ – pure ZnO crystals; ■ – ZnO films deposited on bare glass substrate; x ---- r_{212} tensor component for the ZnO-bare glass interface; x ---- r_{222} for the ZnO-F bare glass interface

Spectral measurements of electrooptics coefficients(see Fig. 7) confirm the theoretical predictions (Table 3) that the doping by F leads to enhanced electrooptics coefficients r_{222}. Moreover, for wavelengths shorter than 420 nm, an increase in the electrooptic coefficient is up to 17 pm/V. Such a huge increase in the Pockels coefficient may open a new era in the design of thin-like electrooptics light modulators for blue lasers. This suggests the important role played by fluorine in the observed spectral dependences of the Pockels effect. The anisotropy observed in the Pockels tensor components confirms the substantial anisotropy of the interface and fluorine contributions. The electrooptics reproduction was better than 1.2%.

Conclusions

We have theoretically predicted and experimentally proved a giant increase (up to one order) in the linear electrooptics ZnO wurtzite films doped by F deposited on the bare glasses. Using BS calculations, as well as molecular dynamics interface optimisation, we predicted that due to insertion of

F one could expect a substantial increase in the charge density non-centrosymmetry on the interface between the bare glass substrate and the appropriate film. We thus demonstrated the possibility of simultaneously using interface non-centrosymmetry, together with the appropriate doping, in order to enhance the electrooptics effect tensor coefficients.

This new phenomenon may provide a new approach for producing competitive miniaturised electrooptics devices. The proposed theoretical approach may be used for looking for new film-like crystalline materials with enhanced second-order nonlinear optical properties.

References

[1] Ahmin A., „J.Am. Ceram. Soc.", **72**, (1989) 369.

[2] Kityk I.V., Smok P., Berdowski J., Lukasierwicz T., Majchrowski A., „Phys. Letters", **280A**, 706 (2001).

[3] Mirtwa R., Gunter P., *Theory of the electrooptics measurements*, „Academic Press", New York, 1982.

[4] Galli G., Martin R.M., Car R., Parinello M, „Phys. Rev.", **B42**, (1990) 7470.

[5] Bylnder B.M., Kleinman L., „Phys. Rev.", **B41**, (1990) 7868.

[6] Troullier N., Martins J.L., „Phys. Rev.", **B43**, (1991) 8861.

[7] Hill N.A., Waghmare U., „Phys. Rev.", **62B**, (2000) 8802.

[8] Asahi R., Mannstadt W., Freeman A.J., „Phys. Rev.", **59B**, (1999) 7486.

[9] Canning A., Mannstadt W., Freeman A.J., „Comput. Phys. Communicat.", **130**, (2001) 233.

[10] Fu H., Zunger A., „Phys. Rev.", **B55**, (1997) 1642.

[11] Malachowski M., Kityk I.R., Sahraoui B., „Phys. Status Solidi", (1999).

[12] Sahraoui B., Kityk I.V., Nguyen Phu X., Hudhomme P., Gorgues A., „Phys. Rev.", **B59**, (1999) 9229.

[13] Kityk I.V., Kasperczyk J., Andrievskii B.V., „Phys. Letters", **A216**, (1996) 161.

[14] Chadi D.J., Cohen M.L., „Phys. Rev.", 8B, (1973) 5747.

[15] Buda F., Kohanoff J., Parrinello M., „Phys. Rev. Lett.", **69**, (1992) 1272.

[16] Persson C., Lindefelt U., „J.Appl.Phys.", **82**, (1997) 5496.

[17] Bachelet G.B., Hamann D.R., Schluter M., „Phys. Rev.", **B26** (1982) 4199.

[18] Louie S.G., Froyen S., Cohen M.L., „Phys. Rev.", **B26**, (1982) 1738.

[19] Blochl P.E., Jepsen O., Andersen O.K., „Phys. Rev.", **B49**, (1994) 16223.

[20] Gavrilenko V.I., Frolov S.I., Klyui N.I., „Physica", **B185**, (1993) 394.

I.V. KITYK[1], J. BERDOWSKI[1] J. EBOTHE

Anomalously Large Pockels Effect in ZnO-F Single Crystalline Films Deposited on Bare Glass

Summary

Large linear electrooptics (the Pockels effect) of up to 17 pm/V for the wavelength 435 nm has been observed in ZnO films doped by fluorine and deposited on bare glass. In order to describe the phenomenon observed, a complex approach, including self-consistent band structure calculations together with the appropriate molecular dynamics simulations of the interfaces, was applied. The origin of the effect observed is linked to substantial charge density non-centrosymmetry between the wurtzite-like crystalline films and the bare glass substrate, as well as to additional charge density polarisation caused by the fluorine.